

Serveur Académique Lausannois SERVAL serval.unil.ch

Author Manuscript

Faculty of Biology and Medicine Publication

This paper has been peer-reviewed but does not include the final publisher proof-corrections or journal pagination.

Published in final edited form as:

Title: An unexpected role of semaphorin3a-neuropilin-1 signaling in lymphatic vessel maturation and valve formation.

Authors: Jurisic G, Maby-El Hajjami H, Karaman S, Ochsenbein AM, Alitalo A, Siddiqui SS, Ochoa Pereira C, Petrova TV, Detmar M

Journal: Circulation research

Year: 2012 Aug 3

Volume: 111

Issue: 4

Pages: 426-36

DOI: 10.1161/CIRCRESAHA.112.269399

In the absence of a copyright statement, users should assume that standard copyright protection applies, unless the article contains an explicit statement to the contrary. In case of doubt, contact the journal publisher to verify the copyright status of an article.



Published in final edited form as:

Circ Res. 2012 August 3; 111(4): 426–436. doi:10.1161/CIRCRESAHA.112.269399.

An unexpected role of semaphorin3A/neuropilin-1 signaling in lymphatic vessel maturation and valve formation

Giorgia Jurisic^{1,*}, H el ene Maby-El Hajjami^{2,*}, Sinem Karaman¹, Alexandra M. Ochsenbein¹, Annamari Alitalo¹, Shoib S. Siddiqui¹, Carlos Ochoa Pereira¹, Tatiana V. Petrova², and Michael Detmar¹

¹Institute of Pharmaceutical Sciences, Swiss Federal Institute of Technology, ETH Zurich, 8093 Zurich, Switzerland ²Division of Experimental Oncology CePO, CHUV and University of Lausanne, 1066 Epalinges, Switzerland

Abstract

Rationale—Lymphatic vasculature plays important roles in tissue fluid homeostasis maintenance and in the pathology of human diseases. Yet, the molecular mechanisms that control lymphatic vessel maturation remain largely unknown.

Objective—We analyzed the gene expression profiles of *ex vivo* isolated lymphatic endothelial cells to identify novel lymphatic vessel expressed genes and we investigated the role of Sema3A and neuropilin-1 (Nrp-1) in lymphatic vessel maturation and function.

Methods and results—Lymphatic and blood vascular endothelial cells from mouse intestine were isolated using fluorescence-activated cell sorting and transcriptional profiling was performed. We found that the axonal guidance molecules Sema3A and Sema3D were highly expressed by lymphatic vessels. Importantly, we found that the semaphorin receptor Nrp-1 is expressed on the perivascular cells of the collecting lymphatic vessels. Treatment of mice *in utero* (E12.5-E16.5) with an antibody that blocks Sema3A binding to Nrp-1, but not with an antibody that blocks VEGF-A binding to Nrp-1, resulted in a complex phenotype of impaired lymphatic vessel function, enhanced perivascular cell coverage and abnormal lymphatic vessel and valve morphology.

Conclusions—Together, these results reveal an unanticipated role of Sema3A/Nrp-1 signaling in the maturation of the lymphatic vascular network likely via regulating the perivascular cell coverage of the vessels thus affecting lymphatic vessel function and lymphatic valve development.

Keywords

Lymphatic vessels; Neuropilin-1; Semaphorin 3A; pericytes; lymphatic valve

Introduction

The lymphatic vascular system has important functions in tissue fluid homeostasis, immune surveillance and dietary lipid absorption in the intestine¹. Impairment of lymphatic vessel

Correspondence and reprint requests: Michael Detmar, M.D., Institute of Pharmaceutical Sciences, Swiss Federal Institute of Technology, ETH Zurich, Wolfgang-Pauli-Str. 10, HCI H303, CH-8093 Zurich, Switzerland, Tel.: ++41-44-633-7361, Fax: +41-44-633-1364, michael.detmar@pharma.ethz.ch.

*These authors contributed equally to this work

Disclosures

The authors declare no conflict of interest.

development and function leads to a number of human lymphedema syndromes, and activation of lymphatic vessels plays an important role in chronic inflammation and in tumor metastasis²⁻⁵. Despite these important functions, basic research into the molecular control of lymphatic system development has been initiated rather recently, and our knowledge of the molecular pathways involved remains limited. Lymphatic vessels first arise during mid-gestation from the existing veins where a subpopulation of endothelial cells (ECs) buds and migrates to form the primitive lymph sacs, which in mice develop into a network of lymphatic vessels by day E14.5⁶. The maturation of the lymphatic vessel network continues into the first postnatal days and involves the formation of the larger collecting lymphatic vessels. The collecting lymphatic vessels acquire a sparse coverage by smooth muscle cells (SMCs) - which is absent from lymphatic capillaries - as well as intraluminal valves that prevent lymph backflow during contraction of the collecting vessels⁷. Recent developmental studies in knock-out mice have revealed several genes, in particular FOXC2, ephrinB2 and integrin-alpha 9⁷⁻⁹, that play important roles in the maturation of collecting lymphatic vessels and in lymphatic valve development. Gene expression profiling studies of cultured human lymphatic (LECs) versus blood vascular endothelial cells (BECs) have been instrumental in identifying novel molecular players that mediate lymphatic development and function¹⁰⁻¹². However, cultured cells lack the distinct cues from the tissue microenvironment^{13, 14}. To address this issue, we have performed a comprehensive gene expression profiling of mouse LECs and BECs that were isolated by high-speed cell sorting directly from mouse tissue. We found that several semaphorin family members showed a distinct expression pattern in blood versus lymphatic vessel endothelium. The semaphorins represent a family of classical axon guidance cues¹⁵ that interact with neuropilin receptors, single-pass membrane proteins with separate domains for semaphorin and vascular growth factor binding¹⁶.

We report that the axonal guidance genes semaphorin 3A (Sema3A) and Sema3D are expressed by lymphatic vessels *in vivo*. Importantly, we found that the semaphorin receptor neuropilin-1 (Nrp-1) is expressed on perivascular cells that sparsely cover the lymphatic vessels throughout the vessel development, and on the collecting lymphatic vessel valves postnatally. Treatment of mice *in utero* with an antibody that blocks Sema3A binding to Nrp-1, but not with an antibody that blocks VEGF-A binding to Nrp-1, resulted in reduced lymphatic vessel function, abnormal morphology of the collecting lymphatic vessels and valves, and aberrant SMC coverage of lymphatic vessels. Together, these results reveal an unanticipated role of Sema3A/Nrp-1 signaling in the maturation of the lymphatic vascular network.

Methods

An expanded Methods section is available in the Online 'Supplemental Material' at <http://circres.ahajournals.org>.

Microarray analysis of ex vivo isolated colon LECs and BECs

Eight-weeks-old C57BL/6J mice were used to obtain colon tissue for the *ex vivo* cell isolation of endothelial cells as previously described¹⁷. Briefly, tissue was enzymatically digested, single-cell suspensions prepared and immunostained with endothelial and leukocyte markers. FACS was performed using a FACSAria and the FACSDiva software (BD Biosciences). Animal experiments were approved by the Kantonales Veterinaeramt Zurich.

Cells were sorted directly into RLT Plus lysis buffer (Qiagen) supplemented with β -mercaptoethanol. RNA was extracted with the RNeasy Plus Micro kit (Qiagen). Amplification of RNA was performed with the Whole Transcriptome-Ovation Pico RNA

Amplification System (NuGEN Technologies, San Carlos, CA). Biotin-labeled cDNA targets were hybridized to GeneChip Mouse Genome 430 2.0 arrays and arrays scanned according to manufacturer's protocol (Affymetrix Inc., Santa Clara, CA). Quality control and summarization based on the MAS5.0 algorithm^{18, 19} were performed in R using the *simpleaffy* package of BioConductor^{20, 21}. Lists of differentially expressed probe sets were produced with pairwise comparisons with pairs defined as LECs and BECs from the same animal. Differentially expressed genes were selected if they passed t-test criteria ($p < 0.01$) and showed at least 2-fold changes between the two groups. All experiments were designed and all information was compiled in compliance with MIAME guidelines²². The array data have been deposited in the National Center for Biotechnology Information (NCBI) Gene Expression Omnibus (GEO) and are accessible through GEO Series accession no. GSE22034.

Quantitative real-time PCR

Taqman Gene Expression Master Mix and assays (Applied Biosystems, Foster City, CA) were used to determine the expression levels of VEGFR1 (Mm_01210866_m1), podoplanin (Mm00494716_m1), LYVE-1 (Mm01280692_m1), Nrp-1 (Mm01253206_m1) and Nrp-2 (Mm00803099_m1) in sorted cells. Duplex reactions with beta-actin (4352341E) as endogenous control were run under standard conditions. Power SYBR Green PCR Master Mix (Applied Biosystems) and QuantiTect Primer Assays (Qiagen) were used to determine the expression levels of Sema3A (QT00173971), Sema3D (QT00125874) and Sema3G (QT1160887) with beta-actin as endogenous control (QT01136772). RNA was extracted from primary human dermal microvascular LECs, BECs¹⁰, HUVECs (ScienCell, Carlsbad, USA), human coronary artery endothelial cells (HCAECs) and pericytes (PromoCell, Heidelberg, Germany) with the RNeasy Micro kit (Qiagen) and transcribed to cDNA using the High Capacity cDNA Reverse Transcription Kit (Applied Biosystems). QuantiTect Primer Assays for human Sema3A (QT00040936), Sema3D (QT00037023) and beta-actin primers (forward: 5'-TCACCGAGCGGGCT-3', reverse: 5'-TAATGTCACGCACGATTTC-3') and TaqMan gene expression assays for Nrp-1 (Hs00826128_m1) and CD31 (Hs00169777_m1) were used. A 7900HT Fast Real-Time PCR System (Applied Biosystems) was used for all qPCR experiments.

Immunohistochemistry

Serial sections of paraffin-embedded mouse colon were boiled in citric buffer for antigen retrieval. After endogenous peroxidase block, sections were incubated in 1% Triton X-100 (Sigma Aldrich, Munich, Germany) and blocked. Immunostaining was performed with goat anti-Sema3A antibody (C-17, Santa Cruz, Santa Cruz, CA), rabbit anti-LYVE-1 antibody (gift from N. Gale, Regeneron Pharmaceuticals, Tarrytown NY) or control goat IgG, followed by biotin-labeled secondary antibodies (Vector, Burlingame, CA). Streptavidin-conjugated peroxidase was used with the AEC kit as a substrate (Vector).

In utero treatment of mice

Timed pregnancies were set up in FVB/N wild type mice. On days E12.5, E14.4 and E16.5 the pregnant females (3 per group) received intraperitoneal injections of 1.2 mg of anti-Nrp-1A antibody, anti-Nrp-1B antibody^{23, 24} or the control mouse IgG antibody. Neonatal mice were collected for analysis at day P5.5.

Lymphatic vessel tracing

Approximately 3 μ l of 5 mg/ml FITC-dextran (Mw ~2000 kDa; Invitrogen) was injected into the forelimb footpad of anaesthetized P5.5 mice (n=8 per group). After 2 min, forelimb lymphatic vessels were imaged noninvasively using a stereomicroscope Lumar.V12 and

AxioCam digital camera (Zeiss, Jena, Germany). After 15 min, the pups were sacrificed, the overlying skin was removed and the lymphatic vessels were imaged.

Whole-mount staining

Intestines with attached mesentery were collected from embryos or neonatal mice and fixed in 4% PFA. Tissue was blocked for unspecific binding and permeabilized with Triton-X. Antibodies used were mouse Cy3-conjugated anti-SMA (Sigma), goat anti-VEGFR3 (AF743, R&D Systems Abingdon, United Kingdom), rabbit anti-Prox1 (gift from K. Alitalo), mouse anti-Nrp-1A²³; goat anti-Nrp-1 (R&D Systems), hamster anti-CD31 (2H8 clone, Millipore, Billerica, MA, USA), goat anti-integrin-alpha 9 (R&D Systems), mouse anti-FNIIIIEA (clone FN-3E2, Sigma), rat anti-mouse CD31 (clone MEC 13.3, BD Biosciences), and AlexaFluor 488, 555, 594 or 647-conjugated secondary antibodies (Invitrogen). Tissues were mounted in Vectashield (Vector) onto chambered coverglasses (Nunc, Rochester NY) for confocal imaging. For quantification of lymphatic valves, total number of valves identified by staining for integrin-alpha9 and FNEIIIA was determined in five mesenteric vessels in 2–3 mice subjected to each type of treatment. One-way ANOVA with Tukey's multiple comparison post test was done to determine statistical significance. Data are shown as mean \pm SD. Whole-mount images were acquired with a LSM 710 FCS confocal microscope and ZEN software (Zeiss) and processed with IMARIS software (Bitplane AG, Zürich, Switzerland).

Pericyte culture and migration

Primary human pericytes isolated from placenta (PromoCell) were cultured according to the manufacturer's recommendations. Pericytes seeded onto chambered coverglass (Nunc) were fixed in 4% PFA and permeabilized with 0.3% Triton-X. Thereafter, primary goat antibody to Nrp-1 (clone C-19, Santa Cruz) or control goat IgG (Abcam, Cambridge, UK) were applied, followed by an AlexaFluor 594 conjugated secondary antibody (Invitrogen) and Hoechst bisbenzimidazole (Invitrogen). Images were acquired with a LSM 710 FCS confocal microscope and ZEN software (Zeiss). Transwell migration assays were performed using polycarbonate, 8 μ m pore size-membrane 24-well plates (Corning Life sciences). 40,000 pericytes at passage 6–7 were seeded in serum-free medium onto the upper side of the insert that was coated with 1 μ g/ml fibronectin (Millipore) on the bottom side and blocked with 0.2% BSA. Cells were allowed to migrate for 3h to the lower chamber containing either 1% FCS alone or also recombinant Sema3A (50, 100 or 200 ng/ml; R&D Systems) and Nrp-1A, Nrp-1B or control mouse IgG antibodies (20 μ g/ml). Non-migrated cells were mechanically removed, migrated cells were stained with Hoechst and 5 random images were taken per insert. Nuclei from 3 wells per condition were counted using the ImageJ program (National Institutes of Health, Bethesda), and one-way ANOVA with Tukey's multiple comparison post test was done to determine statistical significance. Data are shown as mean \pm SEM.

Results

Ex vivo isolation of pure populations of mouse LECs and BECs by high-speed cell sorting

In order to analyze the transcriptional programs of endothelial cells within their tissue microenvironment, we developed a protocol for fast and efficient digestion of mouse colon tissue and high-speed cell sorting of lymphatic and blood vascular endothelial cells. Immunostained colon single-cell suspensions were sorted based on the expression of the pan-endothelial marker CD31, the lymphatic marker podoplanin and the pan-leukocyte marker CD45. Approximately 70% of sorted colon endothelial cells were blood vascular endothelial cells (BECs; CD31⁺CD45⁻podoplanin⁻) and approximately 30% were lymphatic endothelial cells (LECs; CD31⁺CD45⁻podoplanin⁺) (Figure 1A). Total RNA was extracted from these cells and isothermal linear whole transcriptome amplification was applied²⁵. By

qPCR analysis of four animal-matched pairs of *ex vivo* isolated LECs and BECs, the blood vessel marker VEGFR1 and the lymphatic markers podoplanin and LYVE-1 were shown to be consistently differentially expressed in BECs versus LECs (Figure 1B), confirming the specificity of the cell-sorting procedure. The cDNA generated by whole transcriptome amplification of four animal-matched pairs of *ex vivo* isolated LECs and BECs was labeled and hybridized to Affymetrix mouse microarray chips. High quality microarray results were obtained from the small number of cells isolated from the mouse colon tissue (1000–2000 LECs and 2000–4000 BECs). The microarray analysis confirmed high expression levels of lineage-specific genes such as podoplanin and Prox1 in LECs, and neuropilin-1 and von Willebrand factor (vWf) in BECs (Table 1, Supplementary tables 1 and 2, GEO Series accession no. GSE22034).

Semaphorin 3 family members and their receptors have a lineage-specific expression pattern in blood vascular and lymphatic endothelium

In addition to known lineage-specific genes, the microarray analysis of *ex vivo* isolated LECs and BECs also revealed lineage-specific expression of genes whose specific expression by LECs or BECs was not previously reported. By microarray analysis we found a more than 450-fold higher expression level of Sema3D and a more than 150-fold higher expression level of Sema3A in LECs compared to BECs. Conversely, Sema3G had a more than 900-fold and Nrp-1 a more than 1200-fold higher expression in BECs than in LECs (Table 1). By real-time qPCR analysis of *ex vivo* isolated cells, we confirmed the high expression levels of Sema3A and Sema3D in LECs, and of Sema3G and Nrp-1 in BECs. In line with reports showing Nrp-2 expression on veins and lymphatic vessels²⁶, comparable expression levels of Nrp-2 were found in LECs and BECs indicating mixed venous and arterial components in the BEC fraction (Figure 2A). We next tested by qPCR the expression levels of Sema3A and Sema3D in cultured human endothelial cells. We found that Sema3A had up to approximately 8-fold and Sema3D up to approximately 18-fold higher expression levels in cultured human dermal microvascular LECs than in BECs, while HCAECs showed low expression levels of both genes (Figure 2B). Immunohistochemical analysis of Sema3A expression in mouse colon tissue confirmed that Sema3A protein is indeed expressed by LYVE-1-positive lymphatic vessels (Figure 2C, arrowheads) but not by LYVE-1-negative, erythrocyte-filled blood vessels (Figure 2C, asterisks).

Neuropilin-1 is expressed by the collecting lymphatic vessel perivascular cells and valves

Nrp-1 is the only currently known receptor for Sema3A. To identify the potential target cells for lymphatic vessel-produced Sema3A, we next performed immunofluorescence analyses of mouse mesenteric vessels at different developmental stages. We found that at E18.5 and at P3 perivascular cells of the collecting vessels - most likely SMCs or pericytes - expressed Nrp-1 (Figure 3A, first and second row, arrowheads). Interestingly at P6, we observed expression of Nrp-1 on the perivascular cells (Figure 3A, third row, arrowheads) and in the lymphatic vessel valves (Figure 3A, third row arrows). Immunofluorescence analyses of whole-mount preparations of P7 mouse mesentery, stained for Nrp-1 and the lymphatic markers Prox1 and VEGFR3 confirmed that besides expression on the arteries (Figure 3B, asterisk), Nrp-1 is expressed in the lymphatic valves – characterized by a stronger expression of VEGFR3 and Prox1 than the surrounding non-valve associated lymphatic endothelium (Figure 3B, arrowheads). These results indicate that earlier in the development of collecting lymphatic vessels lymphatic endothelium secreted Sema3A is affecting the perivascular cells, while at the later stages lymphatic valve cells might be affected.

***In utero* blockade of Sema3A binding to Nrp-1 results in decreased lymphatic vessel function and lymphatic vessel morphological changes**

We next investigated whether the interaction of Sema3A expressed by lymphatic vessels with its receptor Nrp-1 on perivascular cell and on the lymphatic valves might play a functional role during lymphatic vascular development. To this end, we treated pregnant female FVB/N mice with antibodies that block Nrp-1 ligand binding. We used the anti-Nrp-1A antibody which specifically blocks the binding of Sema3A to Nrp-1, as well as the anti-Nrp-1B antibody which specifically blocks the binding of VEGF-A to Nrp-1^{23, 24}. Antibodies or control IgG were injected between E12.5 and E16.5 - time points when the lymphatic vascular network is maturing and when lymphatic valves start to form, while most of the blood vascular development is already completed. Litter sizes were normal in all treatment groups and no gross morphological abnormalities were observed in close examinations of the offspring. Problems with motor function and coordination were not observed in any of the treatment groups, excluding major effects of the treatment on the nervous system. Pups treated with the anti-Nrp-1A antibody had mildly reduced body weight when compared with control and anti-Nrp-1B-treated pups (Online Figure I).

We next analyzed whether the blockade of Sema3A binding to Nrp-1 might affect the function of collecting lymphatic vessels. To this end, we injected large molecular weight FITC-dextran into the forelimb fat pads of treated and control pups at day P5.5. In control pups, FITC-dextran filled the deep large collecting vessel (Figure 4A, arrowhead) - ranging from the foot to the brachial region - already after a few minutes, rendering it visible through the skin. In contrast, in 5 out of 8 anti-Nrp-1A treated pups, the injected FITC-dextran was drained through the superficial lymphatic vessel network (Figure 4A, arrows). This alternative route of draining suggests that the collecting lymphatic vessels do not function properly in the absence of the Sema3A signal.

To characterize the lymphatic vessel defects we performed immunofluorescence analysis of the treated mice mesentery. Under normal conditions, at day P5.5 the mesenteric collecting lymphatic vessels follow the branches of the mesenteric vein and artery as tubes with an even diameter that is interrupted by subtle constrictions where the lymphatic valves are located (Figure 4B, first and second row, Online Figure II A, first row). Such normal vessel morphology was observed in mice that were treated *in utero* with control IgG and in mice treated *in utero* with anti-Nrp-1B (which blocks VEGF-A binding to Nrp-1). Importantly, in the anti-Nrp-1A-treated group (blockade of Sema3A binding to Nrp-1), a high proportion (55.5%) of offspring had irregularly shaped collecting lymphatic vessels at day P5.5 (Figure 4B, third row, arrows; Online Figure II A, rows 2 to 4, arrowheads).

Large blood vessels in the mesentery, characterized by strong CD31 expression, were not affected in any of the treatment groups (Figure 4B), most likely because development of these vessels was completed before day E12.5. It is of interest that we found fewer blood vessel capillaries in anti-Nrp-1B treated pups at day P5.5 (Online Figure III A and B), indicating that the formation of smaller blood vessels is impaired when VEGF-A binding to Nrp-1 is blocked, in line with previously reported effects of this antibody²⁴. We also analyzed vascular remodeling in the retina at day P5.5. We found no differences between the control group and the anti-Nrp-1A group (Online Figure III C, D and E), in agreement with previously reported results with this antibody at this time point²⁴.

After *in utero* blockade of Sema3A binding to Nrp-1, smooth muscle cells aberrantly cover lymphatic vessels

While blood vessels are densely covered by smooth muscle cells (SMCs), initial lymphatic vessels lack SMC coverage and collecting lymphatic vessels acquire only sparse SMC

coverage - especially in the valve areas that are normally devoid of SMCs⁷. The expression of Nrp-1 by perivascular cells of the developing lymphatic vessels (Figure 3A) prompted us to investigate whether aberrant SMC coverage might have contributed to the abnormal morphology of collecting lymphatic vessels when *Sema3A* binding to Nrp-1 was blocked. Thus, we studied the expression of alpha-smooth muscle actin (α -SMA) in the mesenteries of the treated animals at day P5.5. In agreement with a previous report⁷, at day P5.5 mesenteric lymphatic vessels were sparsely covered by SMCs (Figure 5A, Online Figure II B, first row). Furthermore, the valve areas visible by a strong CD31 signal on the valve leaflets were devoid of SMCs (Figure 5A, arrowheads). This normal phenotype was present in the groups treated with control IgG and with anti-Nrp-1B antibody (Figure 5A, first and second row). Importantly, we found that the collecting lymphatic vessels in anti-Nrp-1A-treated animals had a more pronounced coverage by α -SMA-expressing cells, especially in the valve areas (Figure 5A arrows, Online Figure II B, second row, arrowheads). Detailed examination of the mesenteric lymphatic vessels of the treated animals revealed a significant increase in the number of valve areas covered by SMCs only in the anti-Nrp-1A treated group (Figure 5B).

Cultured primary human pericytes express high levels of Nrp-1 at the mRNA and protein levels (Figure 5C and D). To investigate the possible mechanisms by which lymphatic vessel-produced *Sema3A* might act on perivascular cells, we performed Transwell migration assays and found that significantly fewer pericytes migrated to the lower chamber of the well when *Sema3A* was added to the medium, and that this effect was abrogated by the addition of the anti-Nrp-1A antibody (Figure 5E, $**p<0.01$). These results indicate that *Sema3A*-Nrp1 signal is needed for the regulation of pericyte migration and that its disruption likely leads to the ectopic SMC coverage phenotype observed in mice treated with the anti-Nrp-1A antibody.

Blocking *Sema3A*-Nrp-1 axis indirectly causes lymphatic valve defects

In molecularly defined areas, the LEC monolayer in the collecting lymphatic vessels remodels to form lymphatic valve structures essential for the proper lymphatic draining function²⁷. A closer examination of the lymphatic valves by immunofluorescence analyses revealed that the valve markers integrin- α 9 and fibronectin EIIIA (FNEIIIA) uniformly delineated the valve leaflets in mice treated with control IgG and anti-Nrp-1B antibody (Figure 6A, first and second row). In contrast, integrin- α 9 was mislocalized, and increased and diffuse FNEIIIA expression was present in a significant proportion of valves of mice treated with anti-Nrp1A antibody (Figure 6A, third row). While the total number of valves did not differ between groups (Figure 6B), the anti-Nrp-1A-treated group had a significantly increased number of abnormal valves in the mesentery in comparison with the control group and the anti-Nrp-1B treated group (Figure 6C, $***p<0.001$). These results indicate that the aberrant SMC coverage of the valve areas and the impaired lymphatic flow could result in defective valve morphology.

Discussion

Recently, several axonal guidance molecules have been implicated to also play a role in vascular system development and in the maintenance of proper vascular function¹⁶. In the vascular system, neuropilin receptors have been investigated mainly for their property of binding VEGF family ligands while their semaphorin binding property has been predominantly linked to their functions in the development of the nervous system. The present study for the first time reveals that lymphatic and blood vessels express different members of the semaphorin family, and it identifies *Sema3A* as a novel molecular player in the maturation of the lymphatic vessel network.

In earlier reports, differences in the gene expression between *in vitro* cultured LECs and BECs were analyzed using microarrays^{10, 12}. However, the gene expression signature of cultured endothelial cells significantly differs from their *in vivo* gene expression signature^{13, 14}. Here, we have for the first time analyzed the gene expression profiles of LECs and BECs isolated directly from mouse colon tissue, and we were able to confirm the purity of FACS sorted LECs and BECs by qPCR analysis of vascular lineage-specific genes such as Prox1, podoplanin and VEGFR1. Surprisingly, we found dramatic differences in the endothelial lineage-specific expression levels of several semaphorins since *Sema3A* and *Sema3D* were exclusively detected in lymphatic vessel endothelium. Although *Sema3A* and *Sema3D* were expressed more strongly in cultured lymphatic endothelial cells than in blood vascular endothelial cells, in agreement with a recent report²⁸, the differences in expression levels between LECs and BECs were much more dramatic in *ex vivo* isolated cells. These findings underline the need to perform analyses of endothelial cells directly from tissues and also indicate that microenvironmental cues are needed to maintain the differential gene expression signatures *in vivo*. Our findings of lineage-specific expression of several semaphorin family members suggests that the function of the neuropilin-1 receptor on vessels may also be modulated by binding of semaphorins, in addition to the binding of VEGFs. In our quest to identify a potential role of *Sema3A* in the lymphatic vascular system, we found - by immunofluorescence analyses - that the *Sema3A* receptor *Nrp-1*, in addition to being abundant on arteries, was also expressed on the perivascular cells covering the lymphatic vessels and on the lymphatic valves.

The *Sema3A/Nrp-1* signaling axis is known to provide the repelling cues that ensure the maintenance of boundaries during the pathfinding of axons in the nervous system²⁹. On the other hand *Nrp-1* plays a crucial role in cardiovascular development. Both the general and the endothelial-specific *Nrp-1* deficiency results in embryonic lethality at around mid-gestation^{30, 31}, thus preventing studies of the effects of *Nrp-1* deficiency on the lymphatic vessel maturation. Previously, genetic manipulation and mutagenesis have been used to selectively disrupt *Sema3A-Nrp-1* signal in mice. It was found that neural development was severely affected, whereas no major vascular defects were reported^{31, 32}. It is of interest that only 60% of *Nrp-1^{Sema}* mice survived until P7, and of those, only a few survived to adulthood³¹. Therefore, the collecting lymphatic vessel defects identified in our study could have easily been missed in these earlier studies, while the neuronal defects were avoided in our study by timing the treatment to a late developmental stage. The effects of *Sema3A* deficiency have been studied in several different genetic mouse backgrounds, and the phenotypes ranged from embryonic lethal with vascular defects to viable with neuronal defects^{15, 33}. However a later detailed analysis of *Sema3A* deficient mice revealed no blood vessel defects³⁴. It will be of great interest to create endothelial or even lymphatic endothelial-specific *Sema3A* deficient mice, to specifically investigate *Sema3A* effect on the lymphatic vasculature.

The recent development of two antibodies that specifically block either VEGF-A or *Sema3A* binding to *Nrp-23* provided us with the unique opportunity to separately investigate the effects of these two ligands on lymphatic vascular development. We timed the treatment with the antibodies to avoid the embryonic lethality and the blood vascular defects that are found in the various knock-out mice. Surprisingly, blockade of *Sema3A*, but not of VEGF-A binding to *Nrp-1* had a profound effect on the development of lymphatic vessels, leading to their impaired maturation and function.

We showed that the perivascular cells express *Nrp-1 in vivo* and that *Sema3A* regulates pericyte migration *in vitro* by binding to *Nrp-1*. Based on these results we propose a model in which LEC-secreted *Sema3A* acts on the *Nrp-1* expressing perivascular cells to ensure that they do not cover lymphatic vessels in the valve areas and that they remain sparse

elsewhere on the collecting vessels. Thus, the observed impaired lymphatic flow and abnormal collecting lymphatic vessel morphology in anti-Nrp-1A antibody-treated mice most likely arises due to the ectopic perivascular cell coverage in the valve areas. Similarly, lack of FOXC2, which is first observed on the developing valves at day E15.5 and was shown to interact with NFATc1 to orchestrate the valve formation⁷, was shown to result in abnormal perivascular cell recruitment and subsequent abnormal lymphatic vessel morphology³⁵. Moreover, perivascular cells enable the autonomous lymphatic contraction and flow as a response to tightly regulated nitric oxide production^{36, 37}, so it is conceivable that SMCs positioned on collecting lymphatic vessels are a part of the flow regulating mechanism. After treatment with the anti-Nrp-1A antibody, we observed that the smaller superficial lymphatic vessels filled with FITC-dextran. The underlying mechanism may be that the smaller vessels provide an alternative draining route or that there is a backflow of fluid from the larger vessel into the smaller vessels. Both mechanisms are indicative of impaired lymphatic function.

The animals in which binding of Sema3A to Nrp-1 was blocked displayed a high number of abnormally formed lymphatic valves. Considering that Nrp-1 expression was found in the lymphatic valves only at P6 and 7 (Figure 3A and B) and the treatment was applied *in utero* during the late embryonic development, we conclude that the valve defects most likely did not arise from a direct effect of the blocking antibodies on the developing valve cells, but as a consequence of the changes in the perivascular cell coverage and changes in the lymphatic flow. Indeed, recently it was shown that the correctly established flow in the lymphatic vessels is crucial for the lymphatic valve development³⁸.

Prox1 expression has been shown to be crucial for lymphatic and venous valve specification^{7, 27, 38, 39}. We found that Prox1 levels were not altered in the abnormal lymphatic vessels and valves of anti-Nrp-1A treated mice, indicating that Sema3A-Nrp-1 signal is required at a later time point in valve development and does not affect valve specification.

Importantly, although inhibition of the VEGF-A binding to Nrp-1 did not influence lymphatic vessel development, the formation of small blood vessels was impaired, in agreement with the previously reported effects of this antibody²⁴ - therefore confirming the activity of the antibody.

Class A plexins are neuropilin co-receptors for secreted semaphorins in the nervous system^{40, 41}. Our microarray studies revealed expression of several plexins by LECs and BECs, making it conceivable that also in the lymphatic system plexins transduce signals upon Sema3A binding. It would be of interest, to analyze lymphatic vessel development in mice lacking the class 3 semaphorin plexin co-receptors⁴². Indeed, plexin A1, but not the plexins A2, A3 or A4, is specifically expressed on the lymphatic valves (A. Eichmann, personal communication), where it likely forms a complex with Nrp-1 to transduce a repelling signal.

Taken together, our results identify the Sema3A/Nrp-1 axis as a novel player in lymphatic vascular network maturation, and they point to potential new targets for therapies aimed at modulating lymphatic vessel function.

Supplementary Material

Refer to Web version on PubMed Central for supplementary material.

Acknowledgments

We thank Genentech Inc. for generously sharing their Nrp-1 blocking antibodies with us. We thank C. Fischer for FACS sorting, J. Scholl for excellent technical assistance and S. Proulx and B. Vigl for their help with the experimental set up.

Funding

This work was supported by National Institutes of Health grant CA69184, Swiss National Science Foundation grant 31003A_130627, Krebsliga Schweiz and Krebsliga Zürich, Advanced European Research Council Grant LYVICAM (to M.D.), Lymphatic Research Foundation (to H.M.-E.H.), and Swiss National Science Foundation (PPP0033-114898 to T.V.P.).

Non-standard Abbreviations and Acronyms

BECs	Blood vascular endothelial cells
HUVEC	human umbilical vein endothelial cells
HCAECs	human coronary artery endothelial cells
LECs	lymphatic endothelial cells
SMCs	smooth muscle cells

References

1. Tammela T, Alitalo K. Lymphangiogenesis: Molecular mechanisms and future promise. *Cell*. 2010; 140:460–476. [PubMed: 20178740]
2. Skobe M, Hawighorst T, Jackson DG, Prevo R, Janes L, Velasco P, Riccardi L, Alitalo K, Claffey K, Detmar M. Induction of tumor lymphangiogenesis by vegf-c promotes breast cancer metastasis. *Nat Med*. 2001; 7:192–198. [PubMed: 11175850]
3. Kunstfeld R, Hirakawa S, Hong YK, Schacht V, Lange-Asschenfeldt B, Velasco P, Lin C, Fiebiger E, Wei X, Wu Y, Hicklin D, Bohlen P, Detmar M. Induction of cutaneous delayed-type hypersensitivity reactions in vegf-a transgenic mice results in chronic skin inflammation associated with persistent lymphatic hyperplasia. *Blood*. 2004; 104:1048–1057. [PubMed: 15100155]
4. Baluk P, Tammela T, Ator E, Lyubynska N, Achen MG, Hicklin DJ, Jeltsch M, Petrova TV, Pytowski B, Stacker SA, Ylä-Herttuala S, Jackson DG, Alitalo K, McDonald DM. Pathogenesis of persistent lymphatic vessel hyperplasia in chronic airway inflammation. *J Clin Invest*. 2005; 115:247–257. [PubMed: 15668734]
5. Szuba A, Rockson SG. Lymphedema: Anatomy, physiology and pathogenesis. *Vasc Med*. 1997; 2:321–326. [PubMed: 9575606]
6. Schulte-Merker S, Sabine A, Petrova TV. Lymphatic vascular morphogenesis in development, physiology, and disease. *J Cell Biol*. 2011; 193:607–618. [PubMed: 21576390]
7. Normèn C, Ivanov KI, Cheng J, Zangger N, Delorenzi M, Jaquet M, Miura N, Puolakkainen P, Horsley V, Hu J, Augustin HG, Ylä-Herttuala S, Alitalo K, Petrova TV. Foxc2 controls formation and maturation of lymphatic collecting vessels through cooperation with nfatc1. *J Cell Biol*. 2009; 185:439–457. [PubMed: 19398761]
8. Bazigou E, Xie S, Chen C, Weston A, Miura N, Sorokin L, Adams R, Muro AF, Sheppard D, Makinen T. Integrin-alpha9 is required for fibronectin matrix assembly during lymphatic valve morphogenesis. *Dev Cell*. 2009; 17:175–186. [PubMed: 19686679]
9. Makinen T, Adams RH, Bailey J, Lu Q, Ziemiecki A, Alitalo K, Klein R, Wilkinson GA. Pdz interaction site in ephrinb2 is required for the remodeling of lymphatic vasculature. *Genes Dev*. 2005; 19:397–410. [PubMed: 15687262]
10. Hirakawa S, Hong YK, Harvey N, Schacht V, Matsuda K, Libermann T, Detmar M. Identification of vascular lineage-specific genes by transcriptional profiling of isolated blood vascular and lymphatic endothelial cells. *Am J Pathol*. 2003; 162:575–586. [PubMed: 12547715]

11. Kriehuber E, Breiteneder-Geleff S, Groeger M, Soleiman A, Schoppmann SF, Stingl G, Kerjaschki D, Maurer D. Isolation and characterization of dermal lymphatic and blood endothelial cells reveal stable and functionally specialized cell lineages. *J Exp Med*. 2001; 194:797–808. [PubMed: 11560995]
12. Petrova TV, Makinen T, Makela TP, Saarela J, Virtanen I, Ferrell RE, Finegold DN, Kerjaschki D, Yla-Herttuala S, Alitalo K. Lymphatic endothelial reprogramming of vascular endothelial cells by the prox-1 homeobox transcription factor. *EMBO J*. 2002; 21:4593–4599. [PubMed: 12198161]
13. Amatschek S, Kriehuber E, Bauer W, Reininger B, Meraner P, Wolpl A, Schweifer N, Haslinger C, Stingl G, Maurer D. Blood and lymphatic endothelial cell-specific differentiation programs are stringently controlled by the tissue environment. *Blood*. 2007; 109:4777–4785. [PubMed: 17289814]
14. Wick N, Saharinen P, Saharinen J, Gurnhofer E, Steiner CW, Raab I, Stokic D, Giovanoli P, Buchsbaum S, Burchard A, Thurner S, Alitalo K, Kerjaschki D. Transcriptomal comparison of human dermal lymphatic endothelial cells ex vivo and in vitro. *Physiol Genomics*. 2007; 28:179–192. [PubMed: 17234577]
15. Taniguchi M, Yuasa S, Fujisawa H, Naruse I, Saga S, Mishina M, Yagi T. Disruption of semaphorin iii/d gene causes severe abnormality in peripheral nerve projection. *Neuron*. 1997; 19:519–530. [PubMed: 9331345]
16. Larrivee B, Freitas C, Suchting S, Brunet I, Eichmann A. Guidance of vascular development: Lessons from the nervous system. *Circ Res*. 2009; 104:428–441. [PubMed: 19246687]
17. Jurisic G, Sundberg JP, Bleich A, Leiter EH, Broman KW, Buechler G, Alley L, Vestweber D, Detmar M. Quantitative lymphatic vessel trait analysis suggests *vcam1* as candidate modifier gene of inflammatory bowel disease. *Genes Immun*. 2010; 11:219–231. [PubMed: 20220769]
18. Liu WM, Mei R, Di X, Ryder TB, Hubbell E, Dee S, Webster TA, Harrington CA, Ho MH, Baid J, Smeekens SP. Analysis of high density expression microarrays with signed-rank call algorithms. *Bioinformatics*. 2002; 18:1593–1599. [PubMed: 12490443]
19. Pepper SD, Saunders EK, Edwards LE, Wilson CL, Miller CJ. The utility of *mas5* expression summary and detection call algorithms. *BMC Bioinformatics*. 2007; 8:273. [PubMed: 17663764]
20. Gentleman RC, Carey VJ, Bates DM, Bolstad B, Dettling M, Dudoit S, Ellis B, Gautier L, Ge Y, Gentry J, Hornik K, Hothorn T, Huber W, Iacus S, Irizarry R, Leisch F, Li C, Maechler M, Rossini AJ, Sawitzki G, Smith C, Smyth G, Tierney L, Yang JY, Zhang J. Bioconductor: Open software development for computational biology and bioinformatics. *Genome Biol*. 2004; 5:R80. [PubMed: 15461798]
21. Wilson CL, Miller CJ. Simpleaffy: A bioconductor package for affymetrix quality control and data analysis. *Bioinformatics*. 2005; 21:3683–3685. [PubMed: 16076888]
22. Brazma A, Hingamp P, Quackenbush J, Sherlock G, Spellman P, Stoeckert C, Aach J, Ansorge W, Ball CA, Causton HC, Gaasterland T, Glenisson P, Holstege FC, Kim IF, Markowitz V, Matese JC, Parkinson H, Robinson A, Sarkans U, Schulze-Kremer S, Stewart J, Taylor R, Vilo J, Vingron M. Minimum information about a microarray experiment (miame)-toward standards for microarray data. *Nat Genet*. 2001; 29:365–371. [PubMed: 11726920]
23. Liang W-C, Dennis MS, Stawicki S, Chanthery Y, Pan Q, Chen Y, Eigenbrot C, Yin J, Koch AW, Wu X, Ferrara N, Bagri A, Tessier-Lavigne M, Watts RJ, Wu Y. Function blocking antibodies to neuropilin-1 generated from a designed human synthetic antibody phage library. *J Mol Biol*. 2007; 366:815–829. [PubMed: 17196977]
24. Pan Q, Chanthery Y, Liang W-C, Stawicki S, Mak J, Rathore N, Tong RK, Kowalski J, Yee SF, Pacheco G, Ross S, Cheng Z, Le Couter J, Plowman G, Peale F, Koch AW, Wu Y, Bagri A, Tessier-Lavigne M, Watts RJ. Blocking neuropilin-1 function has an additive effect with anti-vegf to inhibit tumor growth. *Cancer Cell*. 2007; 11:53–67. [PubMed: 17222790]
25. Dafforn A, Chen P, Deng G, Herrler M, Iglehart D, Koritala S, Lato S, Pillarisetty S, Purohit R, Wang M, Wang S, Kurn N. Linear mRNA amplification from as little as 5 ng total RNA for global gene expression analysis. *Biotechniques*. 2004; 37:854–857. [PubMed: 15560142]
26. Herzog Y, Kalcheim C, Kahane N, Reshef R, Neufeld G. Differential expression of neuropilin-1 and neuropilin-2 in arteries and veins. *Mech Dev*. 2001; 109:115–119. [PubMed: 11677062]

27. Srinivasan RS, Oliver G. Prox1 dosage controls the number of lymphatic endothelial cell progenitors and the formation of the lymphovenous valves. *Genes Dev.* 2011; 25:2187–2197. [PubMed: 22012621]
28. Takamatsu H, Takegahara N, Nakagawa Y, Tomura M, Taniguchi M, Friedel RH, Rayburn H, Tessier-Lavigne M, Yoshida Y, Okuno T, Mizui M, Kang S, Nojima S, Tsujimura T, Nakatsuji Y, Katayama I, Toyofuku T, Kikutani H, Kumanogoh A. Semaphorins guide the entry of dendritic cells into the lymphatics by activating myosin ii. *Nat Immunol.* 2010; 11:594–600. [PubMed: 20512151]
29. Kitsukawa T, Shimizu M, Sanbo M, Hirata T, Taniguchi M, Bekku Y, Yagi T, Fujisawa H. Neuropilin-semaphorin iii/d-mediated chemorepulsive signals play a crucial role in peripheral nerve projection in mice. *Neuron.* 1997; 19:995–1005. [PubMed: 9390514]
30. Kawasaki T, Kitsukawa T, Bekku Y, Matsuda Y, Sanbo M, Yagi T, Fujisawa H. A requirement for neuropilin-1 in embryonic vessel formation. *Development.* 1999; 126:4895–4902. [PubMed: 10518505]
31. Gu C, Rodriguez ER, Reimert DV, Shu T, Fritzsich B, Richards LJ, Kolodkin AL, Ginty DD. Neuropilin-1 conveys semaphorin and vegf signaling during neural and cardiovascular development. *Dev Cell.* 2003; 5:45–57. [PubMed: 12852851]
32. Merte J, Wang Q, Vander Kooi CW, Sarsfield S, Leahy DJ, Kolodkin AL, Ginty DD. A forward genetic screen in mice identifies sema3ak108n, which binds to neuropilin-1 but cannot signal. *J Neurosci.* 2010; 30:5767–5775. [PubMed: 20410128]
33. Behar O, Golden JA, Mashimo H, Schoen FJ, Fishman MC. Semaphorin iii is needed for normal patterning and growth of nerves, bones and heart. *Nature.* 1996; 383:525–528. [PubMed: 8849723]
34. Vieira JM, Schwarz Q, Ruhrberg C. Selective requirements for nrp1 ligands during neurovascular patterning. *Development.* 2007; 134:1833–1843. [PubMed: 17428830]
35. Petrova TV, Karpanen T, Norrmen C, Mellor R, Tamakoshi T, Finegold D, Ferrell R, Kerjaschki D, Mortimer P, Yla-Herttuala S, Miura N, Alitalo K. Defective valves and abnormal mural cell recruitment underlie lymphatic vascular failure in lymphedema distichiasis. *Nat Med.* 2004; 10:974–981. [PubMed: 15322537]
36. von der Weid PY, Zawieja DC. Lymphatic smooth muscle: The motor unit of lymph drainage. *Int J Biochem Cell Biol.* 2004; 36:1147–1153. [PubMed: 15109561]
37. Liao S, Cheng G, Conner DA, Huang Y, Kucherlapati RS, Munn LL, Ruddle NH, Jain RK, Fukumura D, Padera TP. Impaired lymphatic contraction associated with immunosuppression. *Proc Natl Acad Sci U S A.* 2011; 108:18784–18789. [PubMed: 22065738]
38. Sabine A, Agalarov Y, Maby-El Hajjami H, Jaquet M, Hagerling R, Pollmann C, Bebbler D, Pfenniger A, Miura N, Dormond O, Calmes JM, Adams RH, Makinen T, Kiefer F, Kwak BR, Petrova TV. Mechanotransduction, prox1, and foxc2 cooperate to control connexin37 and calcineurin during lymphatic-valve formation. *Dev Cell.* 2012
39. Bazigou E, Lyons OT, Smith A, Venn GE, Cope C, Brown NA, Makinen T. Genes regulating lymphangiogenesis control venous valve formation and maintenance in mice. *J Clin Invest.* 2011; 121:2984–2992. [PubMed: 21765212]
40. Cheng HJ, Bagri A, Yaron A, Stein E, Pleasure SJ, Tessier-Lavigne M. Plexin-a3 mediates semaphorin signaling and regulates the development of hippocampal axonal projections. *Neuron.* 2001; 32:249–263. [PubMed: 11683995]
41. Yaron A, Huang PH, Cheng HJ, Tessier-Lavigne M. Differential requirement for plexin-a3 and -a4 in mediating responses of sensory and sympathetic neurons to distinct class 3 semaphorins. *Neuron.* 2005; 45:513–523. [PubMed: 15721238]
42. Tran TS, Rubio ME, Clem RL, Johnson D, Case L, Tessier-Lavigne M, Haganir RL, Ginty DD, Kolodkin AL. Secreted semaphorins control spine distribution and morphogenesis in the postnatal CNS. *Nature.* 2009; 462:1065–1069. [PubMed: 20010807]

Novelty and significance

What is known

- Lymphatic vessels are crucial for maintaining tissue fluid homeostasis and play important roles in human diseases, including lymphedema, chronic inflammation and cancer metastasis.
- Collecting lymphatic vessels are only sparsely covered by pericytes, when compared to blood vessels, and contain intraluminal lymphatic valves that prevent backflow of fluid.
- Recent loss-of-functions studies revealed that the transcription factor FOXC2 and the integrin-alpha 9 play important roles in the control of lymphatic vessel pericyte coverage and lymphatic valve formation.

What new information does this article contribute

- This article provides the first comprehensive analysis of the gene expression profile of lymphatic versus blood vascular endothelial cells isolated directly from mouse tissue and we reveal that several semaphorin 3 family genes show differential expression in these two cell types.
- We show that lymphatic endothelium specifically produces semaphorin3A (Sema3A) which acts on perivascular cells that express the Sema3A receptor neuropilin-1 (Nrp-1).
- Blockade of Sema3A binding to Nrp-1 in vivo resulted in increased pericyte coverage of lymphatic vessels, impaired lymphatic flow, and impaired lymphatic valve formation, revealing an unanticipated function of the Sema3A/Nrp1 axis in lymphatic maturation and function.

Despite the important function of the lymphatic vasculature in physiology, inflammation and cancer, the molecular mechanisms that regulate its function remain poorly characterized. To identify novel molecular players, we analyzed the transcriptional profile of lymphatic versus blood vascular endothelial cells isolated directly from mouse tissue.

We found that Sema3A was specifically expressed by lymphatic endothelium. Sema3A promoted directed migration of perivascular cells that expressed its receptor Nrp-1. In vivo blockade of the Sema3A/Nrp-1 interaction resulted in impaired lymphatic flow, enhanced perivascular cell coverage and abnormal lymphatic vessel and valve morphology.

Our findings, for the first time, identify the murine lymphatic versus blood vascular transcriptome in vivo which strongly differed from results obtained in cultured cells, revealing the importance of microenvironmental cues. The lineage-specific factors identified will aid researchers in studying the function of the lymphatic and blood vascular system in vivo. We also identified an important and unanticipated role of Sema3A/Nrp1 signaling, previously thought to be mainly involved in nervous system development, in the maturation and function of lymphatic vessels.

These findings should have broad future implications for basic vascular research and for the potential development of therapeutic modalities for disorders such as lymphedema and chronic inflammation.

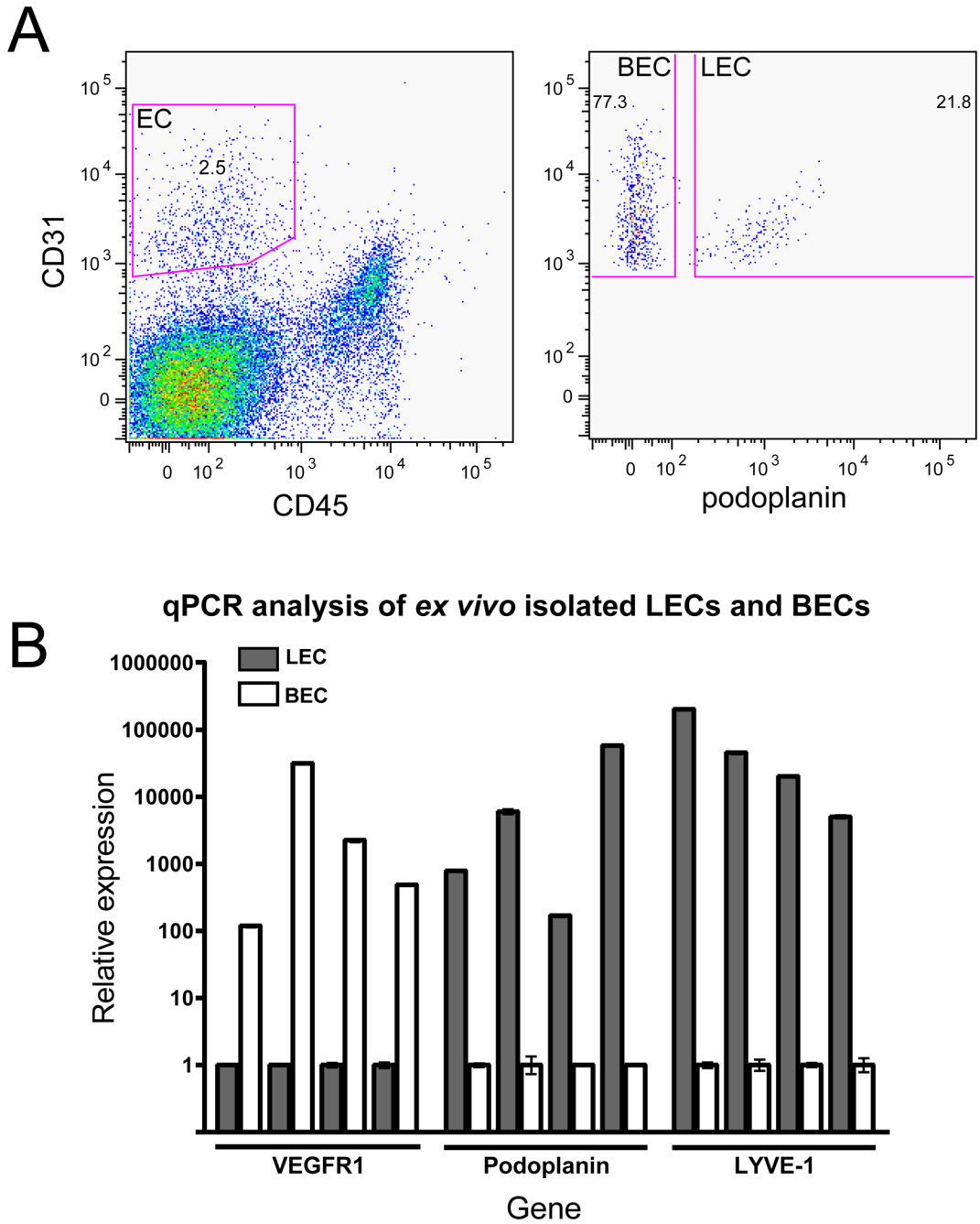


Figure 1. Ex vivo isolation of pure blood vascular and lymphatic endothelial cells from mouse colon tissue by high-speed cell sorting
 (A) Colon single-cell suspensions were immunostained for the pan-endothelial marker CD31, the leukocyte marker CD45 and the lymphatic marker podoplanin. The CD31⁺CD45⁻ population was further separated into podoplanin⁺ LECs and podoplanin⁻ BECs. (B) qPCR for the blood vessel marker VEGFR1 and the lymphatic markers podoplanin and LYVE-1 was performed on sorted LECs and BECs. Four animal-matched pairs of LECs (gray bars) and BECs (white bars) showed consistent differential expression levels. Beta-actin was used for normalization of the expression levels. Error bars show standard deviation.

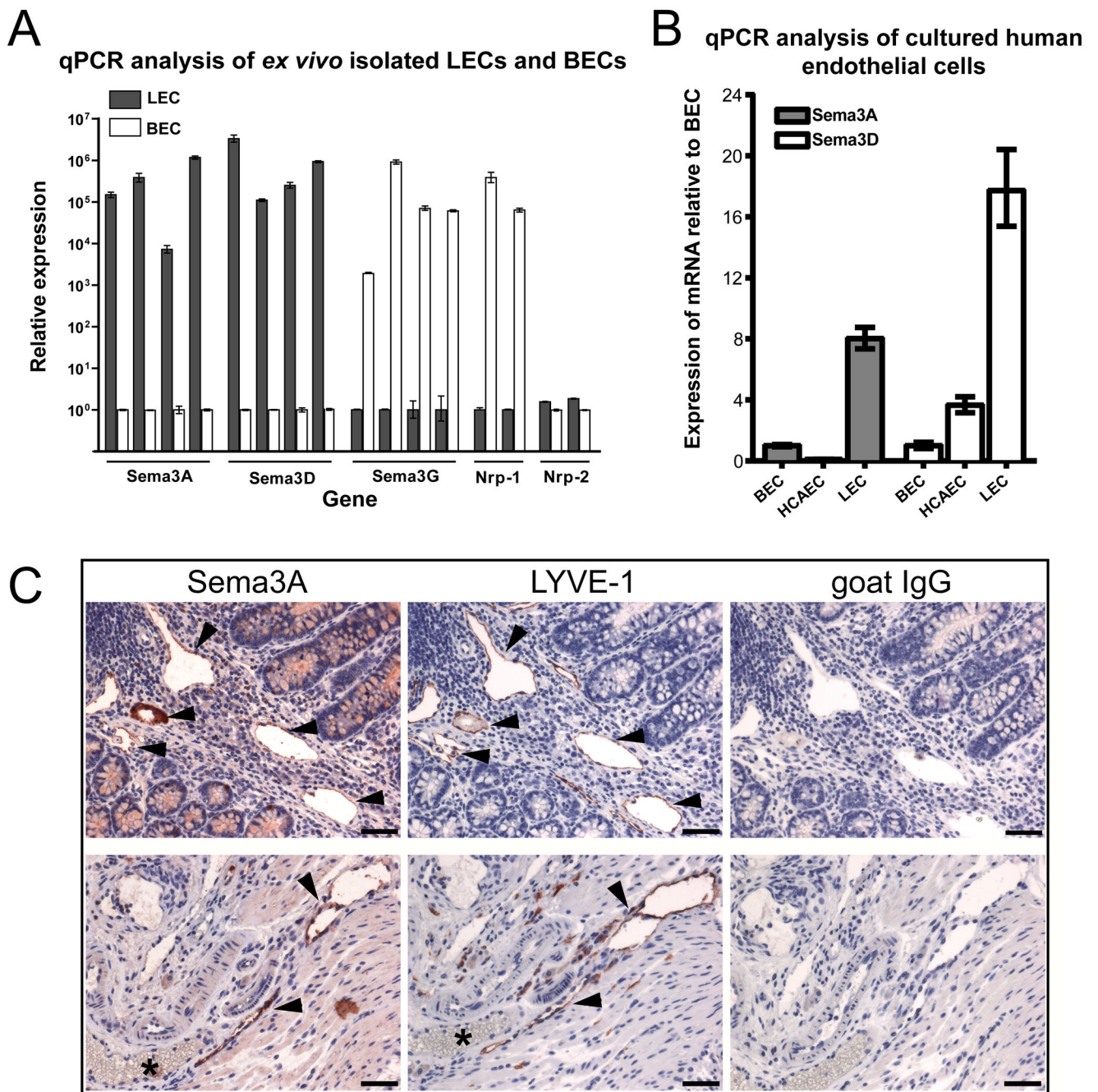


Figure 2. Semaphorin 3 family members are expressed specifically by lymphatic or blood vascular endothelium

(A) Specific expression of Sema3A and Sema3D by lymphatic endothelium, and of Sema3G by blood vascular endothelium, as assessed by qPCR analysis of *ex vivo* isolated mouse LECs and BECs. The semaphorin receptor Nrp-1 was expressed specifically by BECs and Nrp-2 levels were similar in LECs and BECs. (B) Higher expression of Sema3A and Sema3D by cultured human LECs than BECs and HCAECs. Beta-actin was used for normalization of the expression levels. Error bars show standard deviation. (C) Immunohistochemical analysis confirmed the expression of Sema3A in intestinal lymphatic vessels (arrowheads). Serial paraffin sections of mouse colon tissue were immunostained

with antibodies for Sema3A or LYVE-1, or with control goat IgG. Asterisk depicts a LYVE-1-negative blood vessel that is also negative for Sema3A expression. Hematoxylin counterstain. Scale bars: 100 μm .

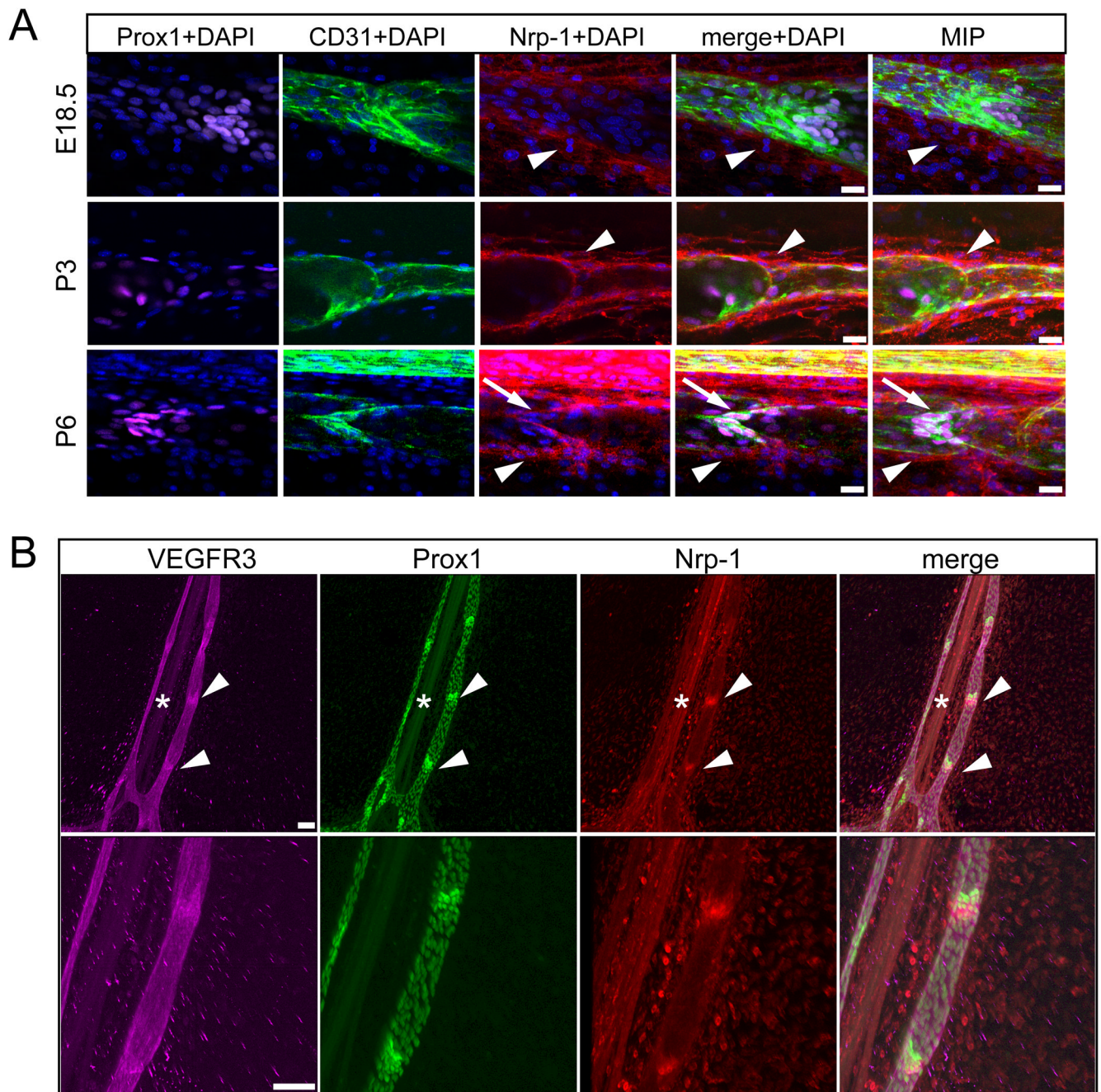


Figure 3. Nrp-1 is expressed on the developing collecting lymphatic vessel perivascular cells and on lymphatic valves

(A) Mouse embryonic mesenteries at E18.5, P3 and P6 were immunostained for Prox1 (magenta), CD31 (green), Nrp-1 (red) and DAPI (blue). The high-magnification single optical slice shows expression of Nrp-1 on lymphatic perivascular cells at E18.5, P3 and P6 (arrowheads). Additionally, at P6 there is an overlap of CD31 (green) and Nrp-1 on the lymphatic valve (arrows). Representative images of 4 mesenteries per stage are shown. MIP (maximum intensity projection) shows a 3D reconstruction of the image. Scale bars: 20 μ m. (B) Immunofluorescence analyses of P7 mouse mesentery whole-mount preparations. The lymphatic markers VEGFR3 (magenta) and Prox1 (green) show stronger expression in the

valve area (arrowheads) than in the remaining lymphatic vessel areas. Nrp-1 (red) signal was found on the artery (asterisks) and in the valve area. The lower panel represents a higher magnification of the upper panel. Images were obtained by confocal microscopy. Scale bars: 100 μm .

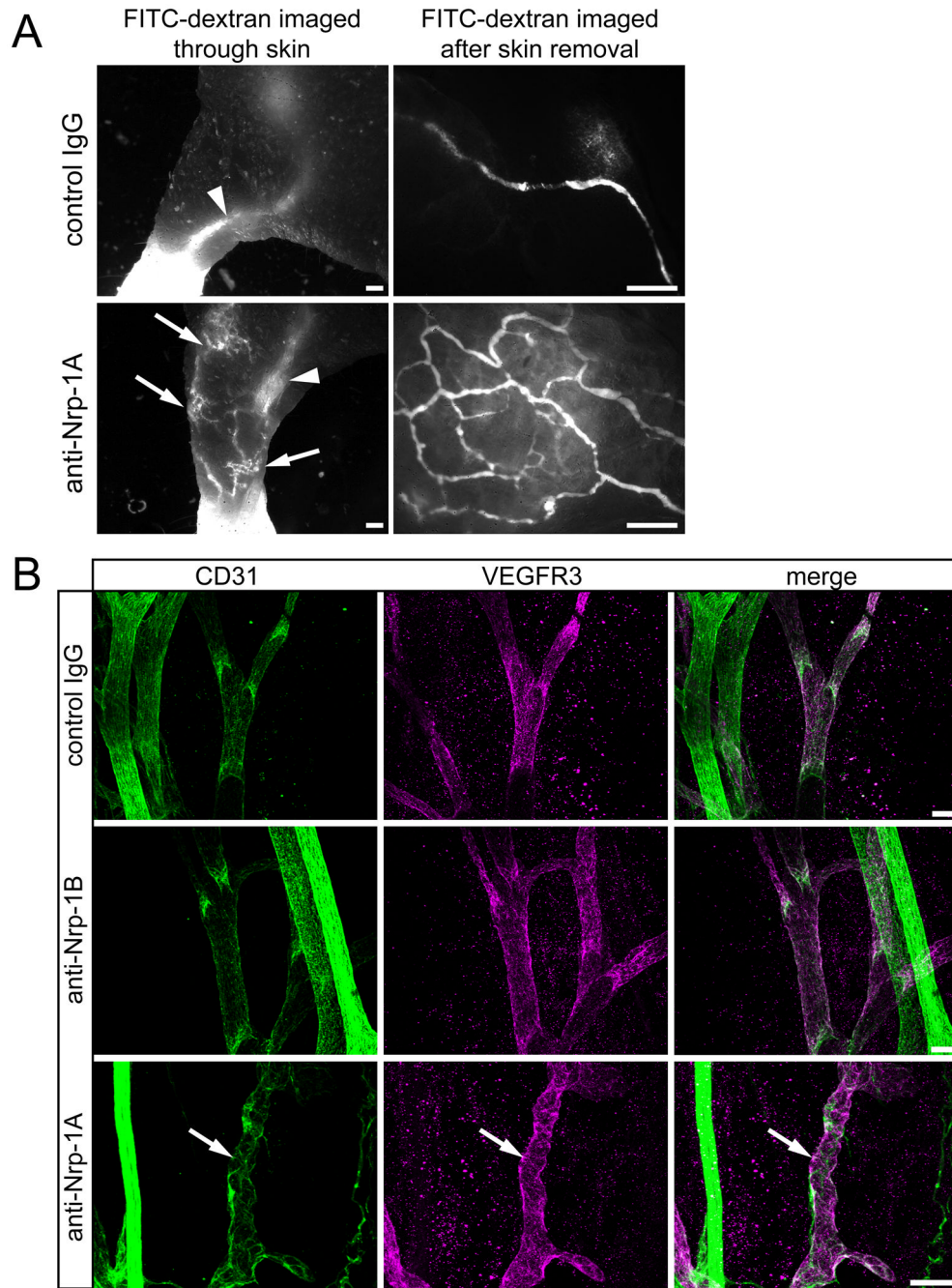


Figure 4. Blockade of Sema3A/Nrp-1 signaling leads to impaired lymphatic vessel function and abnormal morphology of developing collecting lymphatic vessels
 (A) FITC-dextran (2000 kDa) was injected into the forelimb fat pad of control and of anti-Nrp-1A treated pups at day P5.5 to visualize the draining lymphatic vasculature. Low magnification images were taken through the skin and high magnification images were taken after removal of the skin to reveal the lymphatic vessels in more detail. Arrowheads point to the normal route of draining via the deep collecting lymphatic vessels. Arrows point to the alternative draining route via the superficial lymphatic vessel network. Scale bars: 500 μ m. (B) Whole-mount preparations of mesenteries immunostained for CD31 (green) and VEGFR3 (magenta) were analyzed. When compared with control IgG-treated animals (first

row) and anti-Nrp-1B-treated animals (second row), anti-Nrp-1A-treated animals had abnormally formed collecting lymphatic vessels (third row, arrows). Scale bars: 50 μm , n= 13–18 mice per group.

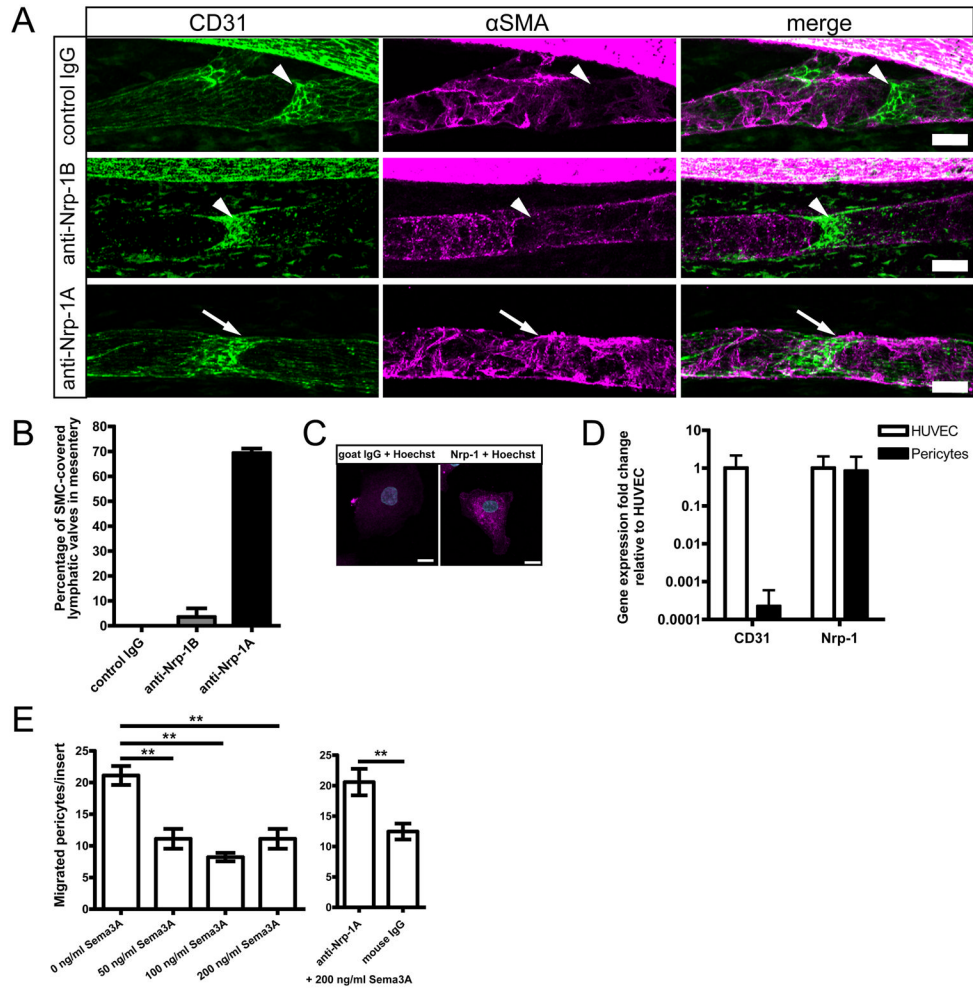


Figure 5. Smooth muscle cells (SMCs) aberrantly cover collecting lymphatic vessels after Semaphorin 3A/Nrp-1 signal blocking, and Semaphorin 3A inhibits migration of Nrp-1 expressing pericytes *in vitro*
 (A) Alpha-smooth muscle actin (α -SMA, magenta) expressing SMCs normally sparsely cover lymphatic vessels and are absent from the valve areas that are visible by a stronger CD31 (green) staining (arrowheads). This phenotype was found in control and in anti-Nrp-1B antibody treated mice at P5.5. Anti-Nrp-1A treatment resulted in excessive coverage of collecting lymphatic vessels by SMCs in the valve areas (arrows). Scale bars: 50 μ m. (B) Quantification of the valve areas covered by SMCs in P5.5 *in utero* treated mice. n= 2–3 mesenteries per group, bars show mean \pm standard deviation. Cultured primary human pericytes express Nrp-1 as assessed by (C) immunofluorescence staining (scale bar: 10 μ m), and by (D) qPCR where pericytes showed low CD31 levels and Nrp-1 levels comparable to those found in HUVEC (mean fold change \pm standard deviation). (E) Semaphorin 3A prevents migration of pericytes to 1% FCS and fibronectin coating. This effect was blocked by incubation with the anti-Nrp-1A antibody but not with control IgG. A representative experiment (out of 3) is shown. Bars show mean values \pm SEM, one-way ANOVA Tukey’s post test. **p<0.01.

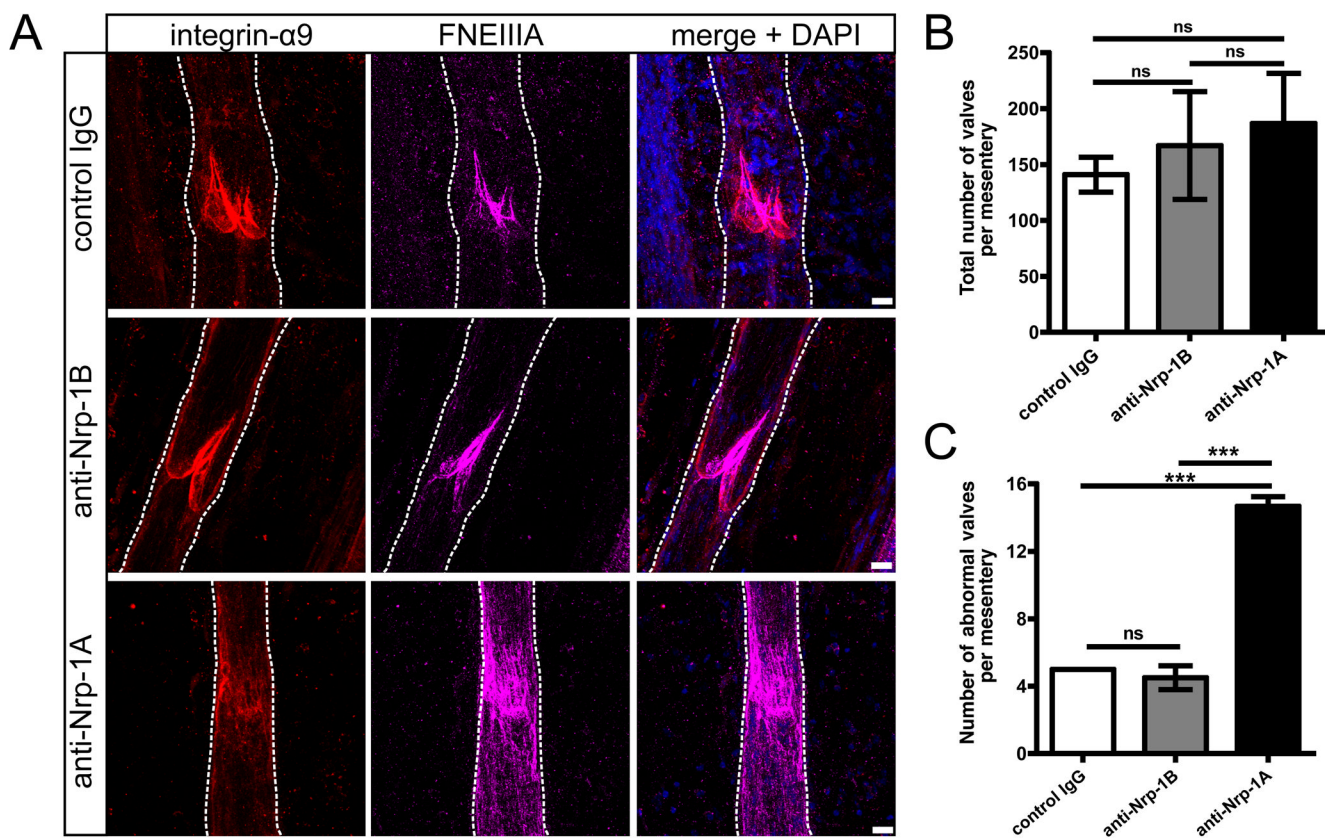


Figure 6. Blocking Sema3A-Nrp-1 signal indirectly causes abnormal lymphatic valve morphology

(A) For lymphatic valve analysis, mesenteries were immunostained for integrin-alpha 9 (red) and fibronectin EIIIA (magenta). The white dotted line outlines the lymphatic vessels. Scale bars: 20 μ m. (B) The total number of valves per mesentery and (C) the number of abnormal valves with excessive FNEIIIA deposition, integrin-alpha 9 mislocalization and ring-shaped leaflets per mesentery were quantified. $n=2-3$ mice per group, bars show mean values \pm SD, one-way ANOVA Tukey's post test. *** $p < 0.001$, ns=not significant.

Table 1
Gene microarray analysis of *ex vivo* isolated mouse intestinal lymphatic versus blood vascular endothelial cells revealed genes that are specifically expressed by lymphatic or blood vessel endothelium

Selected genes with significantly changed expression are shown (complete data can be found at GEO Series accession no. GSE22034 and in Supplementary material).

More strongly expressed in LECs compared to BECs				More strongly expressed in BECs compared to LECs			
Gene name	Probe ID*	fold change**	value***	Gene name	Probe ID*	fold change**	value***
Maf	1456060_at	833.7	6.6E-03	Cxcr4	1448710_at	1375.9	3.4E-04
Gng2	1428157_at	514.0	3.3E-04	Nrp1	1418084_at	1265.8	8.6E-04
Sema3d	1429459_at	484.3	1.5E-04	Sema3g	1435361_at	972.8	2.8E-04
Reln	1449465_at	458.9	3.1E-04	Vegfc	1439766_x_at	660.4	8.4E-04
Pdpr	1419309_at	455.7	1.8E-06	Flt1	1440926_at	622.3	4.6E-04
Lyle1	1429379_at	447.1	6.5E-06	Vwf	1435386_at	202.2	8.6E-04
Ccl21	1419426_s_at	422.3	3.1E-03	Cxcl12	1439084_at	83.0	1.2E-04
Thy1	1423135_at	323.7	7.1E-05	Igfb5	1417534_at	54.0	2.1E-03
Prox1	1437894_at	190.8	1.3E-05	Selp	1449906_at	52.2	2.7E-06
Sema3a	1420416_at	169.3	1.5E-03	Plvap	1418090_at	24.5	5.9E-06
Foxc2	1416693_at	46.9	7.3E-03	Epha4	1421929_at	24.2	2.8E-03
COUP-TFII	1416159_at	33.3	5.6E-04	Sema7a	1422040_at	21.4	2.2E-03
Sema4d	1420823_at	15.5	3.4E-03	Cd34	1416072_at	11.6	9.9E-06
Itga9	1420860_at	12.0	9.1E-03	Efnb1	1418285_at	5.4	8.1E-03
Flt4	1421442_at	4.7	2.0E-04	Plxna2	1455037_at	4.6	2.2E-03

* Probe identification number in Affymetrix GeneChip Mouse Genome 430 2.0

** average fold changes (LEC n=4, BEC n=4)

*** p-value as calculated by unpaired t-test